Title

Upregulation of CD47 Is a Host Checkpoint Response to Pathogen Recognition

Journal

mBio, 11(3)

ISSN

2161-2129

Authors

Tal, Michal Caspi
Dulgeroff, Laughing Bear Torrez
Myers, Lara
et al.

Publication Date

2020-06-30

DOI

10.1128/mbio.01293-20

Peer reviewed

AMERICAN SOCIETY FOR MICROBIOLOGY | mBio®

RESEARCH ARTICLE
Host-Microbe Biology

Upregulation of CD47 Is a Host Checkpoint Response to Pathogen Recognition

Michal Caspi Tal,[a,b] Laughing Bear Torrez Dulgeroff,[a,b] Lara Myers,[c] Lamin B. Cham,[d] Katrin D. Mayer-Barber,[e] Andrea C. Bohrer,[e] Ehydel Castro,[e] Ying Ying Yiu,[a,b] Cesar Lopez Angel,[f] Ed Pham,[f,g] Aaron B. Carmody,[h] Ronald J. Messer,[c] Eric Gars,[i] Jens Kortmann,[j] Maxim Markovic,[a,b] Michaela Hasenkrug,[c] Karin E. Peterson,[c] Clayton W. Winkler,[c] Tyson A. Woods,[c] Paige Hansen,[a,b] Sarah Galloway,[a,b] Dhananjay Wagh,[k,l] Benjamin J. Fram,[g] Thai Nguyen,[g] Daniel Corey,[a,b] Raja Sab Kalluru,[i] Niaz Banaei,[i] Jayakumar Rajadas,[l,m,n] Denise M. Monack,[f] Aijaz Ahmed,[g] Debashis Sahoo,[o,p] Mark M. Davis,[f] Jeffrey S. Glenn,[f,g] Tom Adomati,[d] Karl S. Lang,[d] Irving L. Weissman,[a,b] Kim J. Hasenkrug[c]

[a]Institute for Stem Cell Biology and Regenerative Medicine, Stanford University School of Medicine, Stanford, California, USA
[b]Ludwig Cancer Center, Stanford University School of Medicine, Stanford, California, USA
[c]Laboratory of Persistent Viral Diseases, Rocky Mountain Laboratories, National Institute of Allergy and Infectious Diseases, National Institutes of Health, Hamilton, Montana, USA
[d]Institute of Immunology, Medical Faculty, University of Duisburg-Essen, Essen, Germany
[e]Laboratory of Clinical Immunology and Microbiology, National Institute of Allergy and Infectious Diseases, National Institutes of Health, Bethesda, Maryland, USA
[f]Department of Microbiology and Immunology, Stanford University School of Medicine, Stanford, California, USA
[g]Department of Gastroenterology and Hepatology, Stanford University School of Medicine, Stanford, California, USA
[h]Research Technologies Branch, Rocky Mountain Laboratories, National Institute of Allergy and Infectious Diseases, National Institutes of Health, Hamilton, Montana, USA
[i]Department of Pathology, Stanford University School of Medicine, Stanford, California, USA
[j]Genentech Inc., South San Francisco, California, USA
[k]Stanford Functional Genomics Facility, Stanford University School of Medicine, Stanford, California, USA
[l]Biomaterials and Advanced Drug Delivery Laboratory, Cardio Vascular Institute, Stanford University School of Medicine, Stanford, California, USA
[m]Department of Medicine, Division of Pulmonary and Critical Care Medicine, Stanford University School of Medicine, Stanford, California, USA
[n]Bioengineering and Therapeutic Sciences, UCSF School of Pharmacy, University of California, San Francisco, San Francisco, California, USA
[o]Department of Pediatrics, University of California, San Diego, La Jolla, California, USA
[p]Department of Computer Science and Engineering, Jacobs School of Engineering, University of California, San Diego, La Jolla, California, USA

The following authors contributed equally and have the right to list their name first in their CV: Michal Caspi Tal, Laughing Bear Torrez Dulgeroff, and Lara Myers. Michal Caspi Tal was listed first to acknowledge her supervisor role, followed by Laughing Bear Torrez Dulgeroff given her significant contribution to the final visualization of the data, followed Lara Myers.

Irving L. Weissman and Kim J. Hasenkrug are co-senior authors, and both have the right to list their name last in their CV.

ABSTRACT It is well understood that the adaptive immune response to infectious agents includes a modulating suppressive component as well as an activating component. We now show that the very early innate response also has an immunosuppressive component. Infected cells upregulate the CD47 "don't eat me" signal, which slows the phagocytic uptake of dying and viable cells as well as downstream antigen-presenting cell (APC) functions. A CD47 mimic that acts as an essential virulence factor is encoded by all poxviruses, but CD47 expression on infected cells was found to be upregulated even by pathogens, including severe acute respiratory syndrome coronavirus 2 (SARS-CoV-2), that encode no mimic. CD47 upregulation was revealed to be a host response induced by the stimulation of both endosomal and cytosolic pathogen recognition receptors (PRRs). Furthermore, proinflammatory cytokines, including those found in the plasma of hepatitis C patients, upregulated CD47 on uninfected dendritic cells, thereby linking innate modulation with downstream

Citation Tal MC, Torrez Dulgeroff LB, Myers L, Cham LB, Mayer-Barber KD, Bohrer AC, Castro E, Yiu YY, Lopez Angel C, Pham E, Carmody AB, Messer RJ, Gars E, Kortmann J, Markovic M, Hasenkrug M, Peterson KE, Winkler CW, Woods TA, Hansen P, Galloway S, Wagh D, Fram BJ, Nguyen T, Corey D, Kalluru RS, Banaei N, Rajadas J, Monack DM, Ahmed A, Sahoo D, Davis MM, Glenn JS, Adomati T, Lang KS, Weissman IL, Hasenkrug KJ. 2020. Upregulation of CD47 is a host checkpoint response to pathogen recognition. mBio 11:e01293-20. https://doi.org/10.1128/mBio.01293-20.

Editor Russell Vance, UC Berkeley

Address correspondence to Irving L. Weissman, Irv@stanford.edu, or Kim J. Hasenkrug, khasenkrug@nih.gov.

This article is a direct contribution from Kim J. Hasenkrug, a Fellow of the American Academy of Microbiology, who arranged for and secured reviews by Cornelia Bergmann, Cleveland Clinic, and Anthony Rongvaux, Fred Hutchinson Cancer Institute.

Received 18 May 2020
Accepted 21 May 2020
Published 23 June 2020

adaptive immune responses. Indeed, results from antibody-mediated CD47 blockade experiments as well as CD47 knockout mice revealed an immunosuppressive role for CD47 during infections with lymphocytic choriomeningitis virus and *Mycobacterium tuberculosis*. Since CD47 blockade operates at the level of pattern recognition receptors rather than at a pathogen or antigen-specific level, these findings identify CD47 as a novel potential immunotherapeutic target for the enhancement of immune responses to a broad range of infectious agents.

IMPORTANCE Immune responses to infectious agents are initiated when a pathogen or its components bind to pattern recognition receptors (PRRs). PRR binding sets off a cascade of events that activates immune responses. We now show that, in addition to activating immune responses, PRR signaling also initiates an immunosuppressive response, probably to limit inflammation. The importance of the current findings is that blockade of immunomodulatory signaling, which is mediated by the upregulation of the CD47 molecule, can lead to enhanced immune responses to any pathogen that triggers PRR signaling. Since most or all pathogens trigger PRRs, CD47 blockade could be used to speed up and strengthen both innate and adaptive immune responses when medically indicated. Such immunotherapy could be done without a requirement for knowing the HLA type of the individual, the specific antigens of the pathogen, or, in the case of bacterial infections, the antimicrobial resistance profile.

KEYWORDS CD47, host response, immune checkpoint, innate immunity, pathogen recognition receptors

The earliest immune responses to invasion by pathogenic microorganisms begin with the sensing of pathogen-associated molecular patterns (PAMPs) by pattern recognition receptors (PRRs) such as Toll-like receptors (TLRs). Ligation of PRRs initiates signal transduction pathways that ultimately lead to the activation of broad innate and highly specific adaptive immune responses. Discoveries in recent years have demonstrated that the induction of adaptive immune responses involves not only activation mechanisms but also inhibitory mechanisms or "checkpoints," which regulate immune function at a cellular level to prevent immunopathological damage by overactivated effector responses (1). Antibody (Ab)-mediated blockade of checkpoint molecules such as CTLA4 and PD-1 is being used therapeutically to enhance anticancer immune responses (2, 3), and blockade of CD47 is now in clinical trials to activate macrophage-mediated phagocytosis of cancer cells (4–7), which upregulate CD47 expression as an immune evasion mechanism (8–11).

CD47 is an abundantly expressed transmembrane cell surface glycoprotein that can act as a receptor for thrombospondins, form complexes with integrins, and bind to the inhibitory receptor signal-regulatory protein alpha (SIRPα) (12–14). CD47 binding to SIRPα has emerged as an important innate immune checkpoint by regulating immune cell clearance and inflammatory signaling (6). CD47 engagement of SIRPα results in the phosphorylation of cytoplasmic ITIM motifs by inhibitory protein tyrosine phosphatases, SHP-1 and SHP-2 (15). Given the well-established role of CD47 in cancer cell immune evasion, we investigated whether CD47 expression is modified in other disease contexts, specifically infectious diseases. The CD47-SIRPα axis has immunomodulatory functions that impact phagocytosis, chemokine and cytokine responses, innate and adaptive immune cell homeostasis and activation, T cell killing, and B cell antibody production (15–18).

Viruses have evolved mechanisms to evade host defenses (19) and take advantage of inhibitory signaling pathways for selective advantage. Of interest, poxviruses, which devote many genes toward immune suppression and evasion, encode a CD47 mimic (20). The CD47 mimic of myxomavirus, M128L, can be deleted with no effect on *in vitro* replication, but the deletion mutant loses pathogenicity *in vivo*. This loss of pathogenicity was associated with increased monocyte/macrophage activation (20).

The present study examines CD47 expression in the context of infectious agents that

encode no CD47 mimic. Both mouse and human cells showed a significant upregulation of CD47 upon infection with various pathogens. The results indicated that stimulation of either cytosolic or endosomal PPRs resulted in CD47 upregulation. In addition, inflammatory cytokines present in the serum of hepatitis C virus (HCV)-infected patients could also induce CD47 upregulation, even in the context of no virus. In addition to viruses, clinically relevant bacteria such as *Mycobacterium tuberculosis* induce the upregulation of CD47 that limits host resistance. Our results indicate that CD47 upregulation is a very early innate checkpoint response and that immunological inhibitory mechanisms are activated not only at the effector phase of immune responses but also already at the induction phase of PRR sensing. Thus, CD47 is a promising target for checkpoint therapies against a wide range of infectious diseases.

RESULTS

CD47 expression is upregulated on mouse hematopoietic cells in response to *in vivo* infection. To examine the role of CD47 expression during the innate response to infection, we investigated whether hematopoietic cells upregulated CD47 expression in several unrelated infection models during the first days after infection. We began by analyzing CD47 expression on cells from mice inoculated with Friend virus (FV), a naturally occurring retroviral infection in mice (21). FV primarily infects erythroid progenitor cells in the spleen but can also infect immune cells (22). CD47 was significantly upregulated on several hematopoietic cell lineages from mouse spleens at 3 days postinfection (dpi) compared to cells from naive mice (Fig. 1A). CD47 expression was also analyzed at 2 dpi in mice infected with lymphocytic choriomeningitis virus (LCMV). Compared to naive controls, all of the spleen cell types analyzed showed significantly increased cell surface expression of CD47 (Fig. 1B). A significant upregulation of CD47 expression was also observed in response to LCMV at 3 dpi in a previous report (23). Infections with La Crosse arbovirus were also analyzed at 2 dpi, and we also observed significantly upregulated CD47 expression in hematopoietic spleen cells compared to naive controls (Fig. 1C).

CD47 expression is upregulated on human cells in response to *in vitro* infection. Examination of a publicly available gene expression data set (Gene Expression Omnibus [GEO] accession number GSE147507) from severe acute respiratory syndrome coronavirus 2 (SARS-CoV-2) infection of A549 human lung cells also showed a significant upregulation of CD47 compared to mock-infected controls (Fig. 1D). To determine whether bacterial infection would also upregulate CD47 expression, human peripheral blood mononuclear cells (PBMCs) were examined 24 and 48 h after infection with *Borrelia burgdorferi in vitro*. Multiple PBMC subsets showed significantly upregulated CD47 expression in response to *Borrelia burgdorferi* infection compared to naive cells (Fig. 1E). We also investigated CD47 expression on human PBMCs infected *in vitro* with mCherry-expressing strains of *Salmonella enterica* serovar Typhi. Wild-type *Salmonella* Typhi (Ty2 WT) and *Salmonella* Typhi Δ*fliC* (Ty2 Δ*fliC*), a mutant strain that lacks flagella, were examined. Infections were done by centrifugation to compensate for the lack of motility of the flagellum mutant. Compared to naive cells, mCherry-positive B cells significantly upregulated CD47 expression when infected with wild-type *Salmonella* Typhi for 24 h (Fig. 1F). In contrast, CD47 expression was not significantly upregulated in B cells infected with the mutant strain lacking flagella, *Salmonella* Typhi Δ*fliC* (Fig. 1F). The reduced upregulation of CD47 expression by *Salmonella* Typhi Δ*fliC* compared to wild-type *Salmonella* Typhi suggested that the sensing of pathogen-associated molecular patterns (PAMPs) by pattern recognition receptors (PRRs) might play a role in CD47 upregulation, as flagellin is a potent PAMP recognized by extracellular TLR5 (24) and the NLR family of apoptosis-inhibitory proteins (NAIPs) (25). Overall, the combined *in vivo* and *in vitro* results from multiple pathogen infections in both human and mouse cells indicated that the upregulation of CD47 was a conserved host response possibly related to host sensing mechanisms.

CD47 is upregulated in response to host recognition of pathogens. To determine whether CD47 upregulation was initiated by PRR stimulation, we specifically

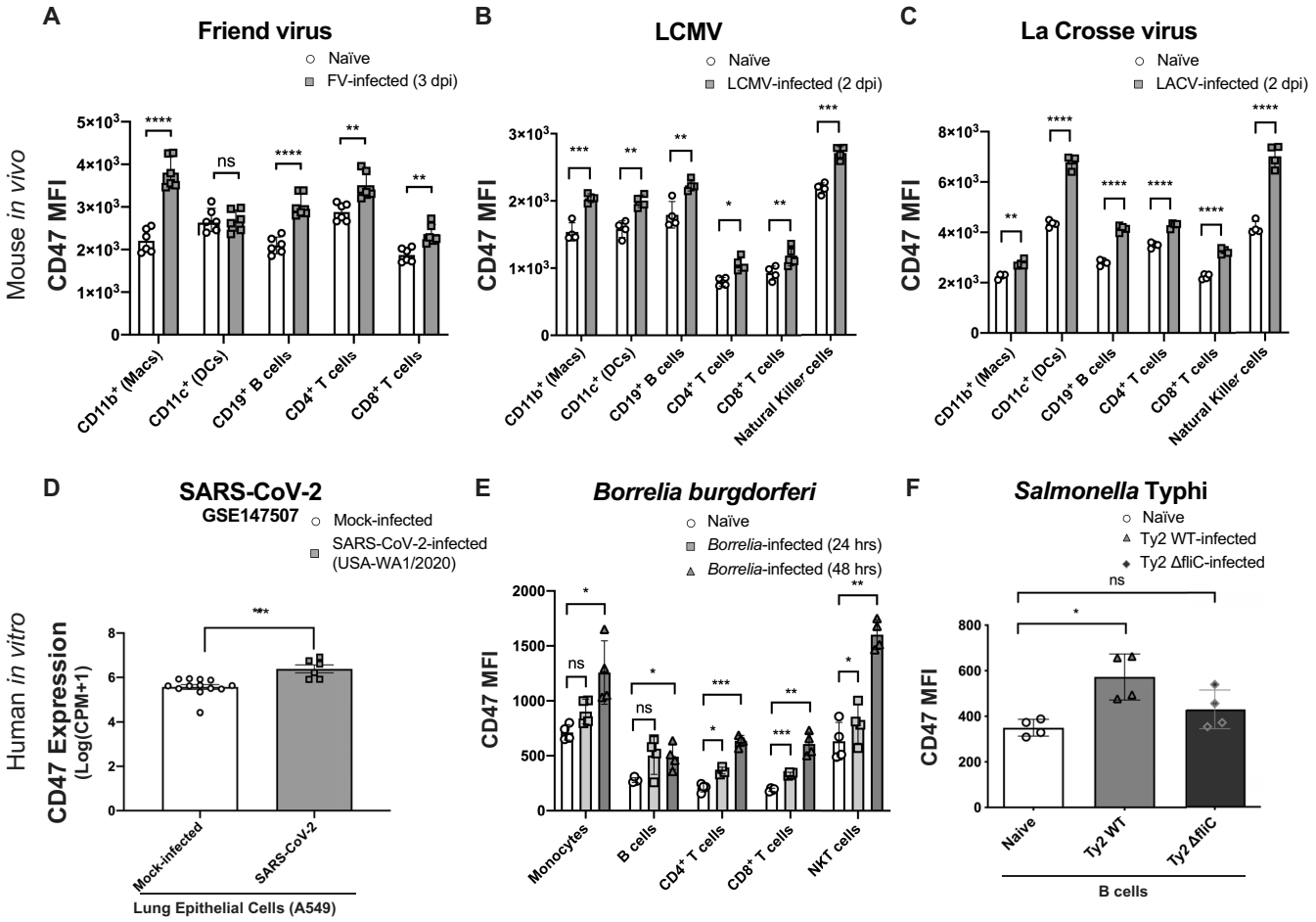

FIG 1 CD47 is broadly upregulated in immune cell types in response to several types of infection. (A and B) Comparison of CD47 median fluorescence intensities (MFI) on splenic hematopoietic cell subsets from naive mice and female (A.BY × C57BL/6)F_1 mice infected intravenously with 2×10^4 SFFU Friend virus at 3 days postinfection (A) or female C57BL/6 mice infected intravenously with 2×10^6 PFU LCMV-WE at 2 days postinfection (B). (C) Female C57BL/6 mice inoculated intraperitoneally with 10^5 PFU La Crosse virus at 2 days postinfection. (D) CD47 expression levels analyzed from the publicly available gene expression data set from SARS-CoV-2 infection of A549 human lung tumor cells (GEO accession number GSE147507) ($n = 10$) comparing mock-infected ($n = 13$) with SARS-CoV-2 (USA-WA1/2020)-infected cells ($n = 6$). (E) Comparison of CD47 MFI on hematopoietic cells from *Borrelia burgdorferi*-GFP-infected human PBMCs 24 and 48 h after *in vitro* infection, compared to naive controls. GFP was used under infection conditions to identify cells with intracellular *Borrelia* infection (shaded). (F) Comparison of CD47 MFI on human CD19+ B cells 24 h after *in vitro* infection with *Salmonella enterica* serovar Typhi strain Ty2 (Ty2 WT) or *Salmonella enterica* serovar Typhi strain Δ*fliC* (Ty2 Δ*fliC*), which lacks flagella, compared to naive controls. Statistical analyses were done by Student's *t* tests for panels A to D and by one-way analysis of variance (ANOVA) with a multiple-comparison posttest for panels E and F (ns [not significant], $P > 0.05$; *, $P < 0.05$; **, $P < 0.01$; ***, $P < 0.001$; ****, $P < 0.0001$). Error bars represent standard errors of the means (SEM).

stimulated PRRs using small-molecule agonists rather than infectious agents. CD47 upregulation on human dendritic cells (DCs) and monocytes was tested *in vitro* using PBMCs stimulated with either muramyl dipeptide (MDP) to activate the bacterial peptidoglycan PRR, nucleotide-binding oligomerization domain-containing protein 2 (NOD2), or CL264 to activate the single-stranded RNA (ssRNA) endosomal PRR, TLR7. Flow cytometry was used to identify cell subsets and measure CD47 expression at 24 h poststimulation. Both human DCs and monocytes responded to either type of PRR stimulation with a significant upregulation of CD47 surface expression (Fig. 2A). We also tested TLR stimulation using a dual TLR7/8 agonist, R848. Since this dual agonist, which also has *in vivo* activity (26), produced dose-dependent upregulation of CD47 on human PBMCs (Fig. 2B), we proceeded to test PRR stimulation in an *in vivo* mouse model. Daily intraperitoneal injections of R848 into mice led to strongly upregulated CD47 expression on both macrophages and DCs isolated from spleens on day 3 (Fig. 2C). Together, these data demonstrated that CD47 was upregulated on both human and mouse immune cells via pathogen-sensing mechanisms. Furthermore, TLR7 stimulation via endosomal uptake indicated that CD47 could be upregulated not only

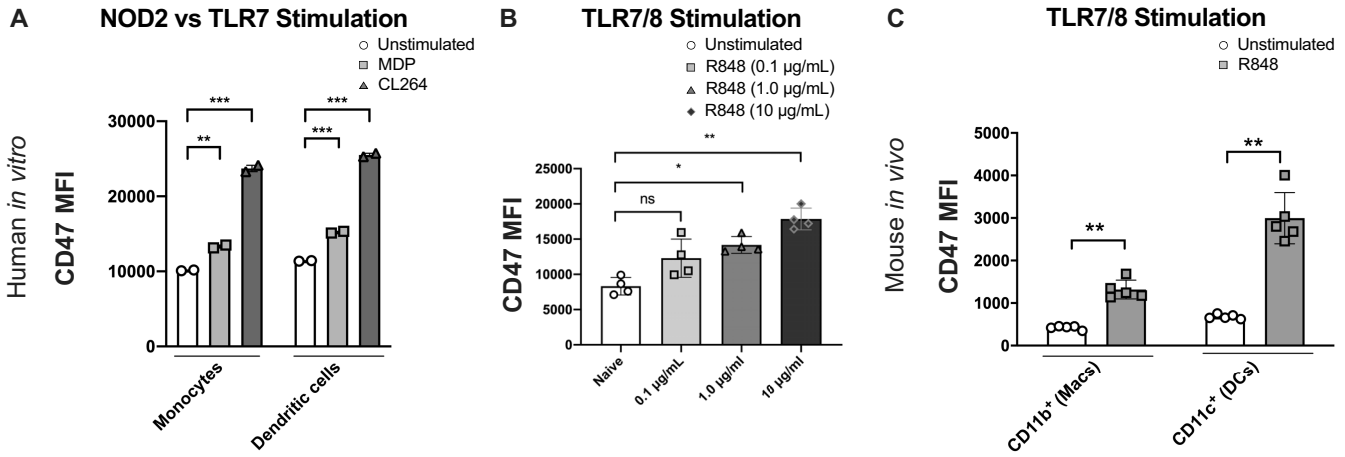

FIG 2 Stimulation of pathogen-associated molecular patterns upregulates CD47 surface expression. (A) MFI of CD47 surface expression on human PBMC monocytes and dendritic cells after 48 h of stimulation with either 1 μg/ml MDP or 1 μg/ml CL264 or with no stimulation. The results are from one of three experiments with two different donors. All 3 experiments showed consistent effects. Statistics were done by a paired two-way *t* test with Bonferroni correction. (B) CD47 MFI on human total PBMCs from 4 separate donors stimulated with titrated concentrations of R848 from 0.1 μg/ml to 10 μg/ml, as indicated, for 48 h. Statistics were done by a paired two-way *t* test with Bonferroni correction. (C) Mice ($n = 5$/group) were injected intraperitoneally with 1 mg/kg R848 for 3 days, and on day 3, splenocytes were isolated and macrophages and DCs were analyzed for CD47 MFI. Statistics were done by an unpaired two-way *t* test. (ns, $P > 0.05$; *, $P < 0.05$; **, $P < 0.01$; ***, $P < 0.001$). Error bars represent SEM.

by infected cells, as would be reflected by cytosolic NOD2 stimulation, but also by surveilling immune cells.

CD47 expression is upregulated during HCV infection *in vivo*. To examine CD47 expression in human viral infection, we first compared transcriptional levels of CD47 from publicly available microarray data (GEO accession number GSE38597) from healthy and hepatitis C virus (HCV) patient liver biopsy specimens. The analysis revealed significantly higher expression levels of CD47 in the liver biopsy specimens from acutely infected HCV patients than for healthy controls (Fig. 3A). We then used cytometry by time of flight (CyTOF) to examine CD47 expression on PBMCs during HCV infection in the context of sofosbuvir (SOF) therapy (27), comparing healthy controls to HCV-infected patients prior to treatment, midway through treatment, and at 6 months posttreatment. Compared to healthy controls, monocytes and DCs from HCV patients demonstrated a sustained upregulation of CD47 at all treatment time points, including the 6-month posttreatment time point (Fig. 3B and C). There were no significant

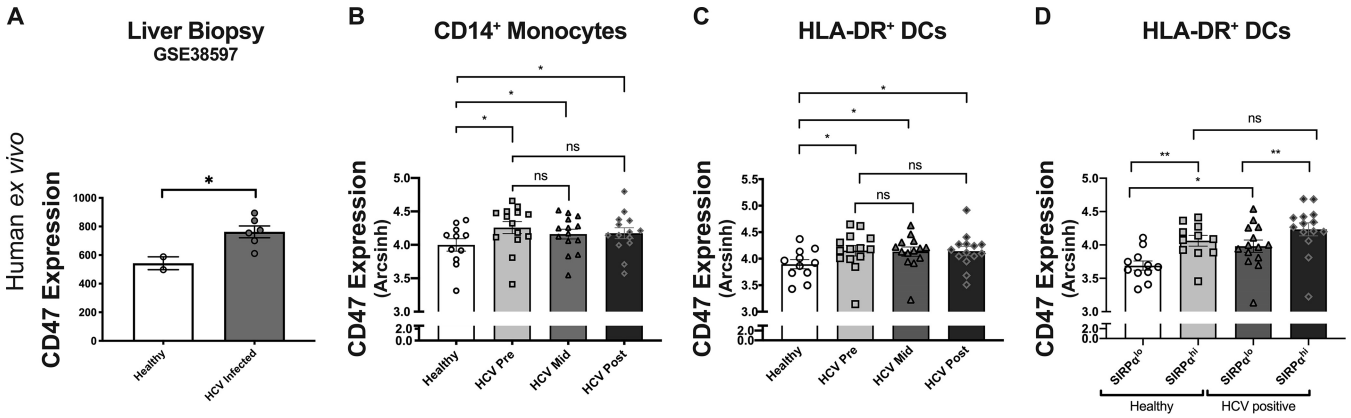

FIG 3 CD47 is involved in innate licensing of adaptive immune responses in HCV patient clinical samples. (A) Comparison of CD47 expression from Affymetrix array profiles of liver biopsy specimens from two healthy controls and six patients with acute HCV infection ($P = 0.03$ by an unpaired two-way *t* test) (NCBI GEO accession number GSE38597). (B and C) Comparison of CD47 expression by CyTOF MFI on CD14$^+$ monocytes (B) and HLA-DR$^+$ DC subpopulations (C) isolated from HCV-infected sofosbuvir-treated patients before the initiation of treatment (Pre), midway through treatment (Mid), and after treatment (Post) compared to healthy controls. (D) Comparison of CD47 expression on SIRPα^{lo} versus SIRPα^{hi} DCs from healthy control and HCV patients. Statistics were done by one-way ANOVA with multiple-comparison posttests (ns, $P > 0.05$; *, $P < 0.05$; **, $P < 0.01$). Error bars represent SEM.

differences between pre-, mid-, and posttreatment CD47 levels in either monocytes or DCs, and all of these time points were significantly different from those for healthy controls (Fig. 3B and C). Conventional dendritic cells (cDCs) are classified into cDC1s and cDC2s, which can be distinguished in part through the specific expression of the CD47 receptor, SIRPα, on cDC2s (28). When we compared CD47 expression levels within SIRPα^{lo} and SIRPα^{hi} DCs, we observed that CD47 expression was highest on SIRPα^{hi} DCs (Fig. 3D). There was no correlation between viral titers and CD47 expression on either monocytes or DC subsets in this patient cohort (see Fig. S1A in the supplemental material). Between healthy controls and pretreatment HCV patients, there was significant CD47 upregulation in SIRPα^{lo} DCs but not in SIRPα^{hi} DCs (Fig. 3D). However, compared to healthy controls, the proportion of SIRPα^{hi} DCs was significantly increased at both pretreatment and midtreatment, which could also contribute to higher CD47 expression levels in DCs (Fig. S1B). Thus, HCV infections were associated with the increased expression of both CD47 and its receptor, SIRPα, on antigen-presenting cells (APCs).

HCV patient plasma-induced CD47 expression *ex vivo*. To determine whether inflammatory factors present in HCV patient plasma could affect CD47 upregulation, we derived DCs from healthy donor monocytes with plasma added from either patients in the HCV patient cohort or healthy controls. We found that monocyte-derived DCs (mDCs) cultured in the presence of HCV patient plasma significantly upregulated CD47 compared to plasma from healthy donors (Fig. 4A). Luminex analysis of patient plasma was used to characterize the inflammatory milieu over the course of HCV infection and treatment. Plasma isolated from patients at the pretreatment time point contained both virus and inflammatory cytokines, indicating that CD47 upregulation could have been due to infection of the DCs. However, plasma isolated from patients at the midtreatment and posttreatment time points contained no detectable virus (data not shown) but still had increased levels of inflammatory cytokines, including tumor necrosis factor alpha (TNF-α), CXCL10, and interferon alpha (IFN-α), compared to healthy controls (Fig. 4B to D). CD47 expression was increased under all HCV patient plasma conditions compared to healthy controls despite undetectable virus at the midtreatment and posttreatment time points. The differences between the pre-, mid-, and posttreatment time points within HCV patients were not statistically significant. These results suggested that cytokines in the inflammatory milieu of HCV patient plasma could upregulate CD47 expression.

To confirm the ability of cytokines to upregulate CD47 surface expression, we performed *in vitro* stimulations of human PBMCs isolated from healthy donors using TNF-α, CXCL10, and IFN-α, as single treatments and in combinations. At 72 h poststimulation, the only single cytokine that induced significant CD47 upregulation was IFN-α (Fig. 4E). Combinations of these inflammatory cytokines enhanced the upregulation of CD47 surface expression, with the triple combination of TNF-α, CXCL10, and IFN-α having the strongest effect (Fig. 4E). These experiments demonstrated that in addition to pathogen recognition, host immune cells could also upregulate CD47 surface expression in response to the inflammatory milieu induced by the pathogen.

Blockade of CD47 signaling enhances antiviral immune responses *in vivo*. To determine the effects of CD47 blockade during a live viral infection, C57BL/6 mice were injected with anti-CD47 (blocking) antibody daily beginning 2 days prior to infection with LCMV. To ascertain whether both anti-CD47-treated and mock-treated animals were equivalently infected, LCMV titers in the spleens and liver were determined at 3 dpi. The analyses showed no significant differences in viral titers at this time point regardless of treatment (Fig. 5A). Anti-CD47 injections were continued through 5 dpi, and plasma virus levels were then measured at 8 and 12 dpi. Significantly reduced viremia levels were observed in anti-CD47-treated mice compared to mock-treated mice at both time points (Fig. 5B). Since it is known that host clearance of LCMV is highly dependent on CD8$^+$ T cell responses (29, 30), it was of interest to determine if CD47 blockade affected those responses. Total CD8$^+$ T cell levels were determined

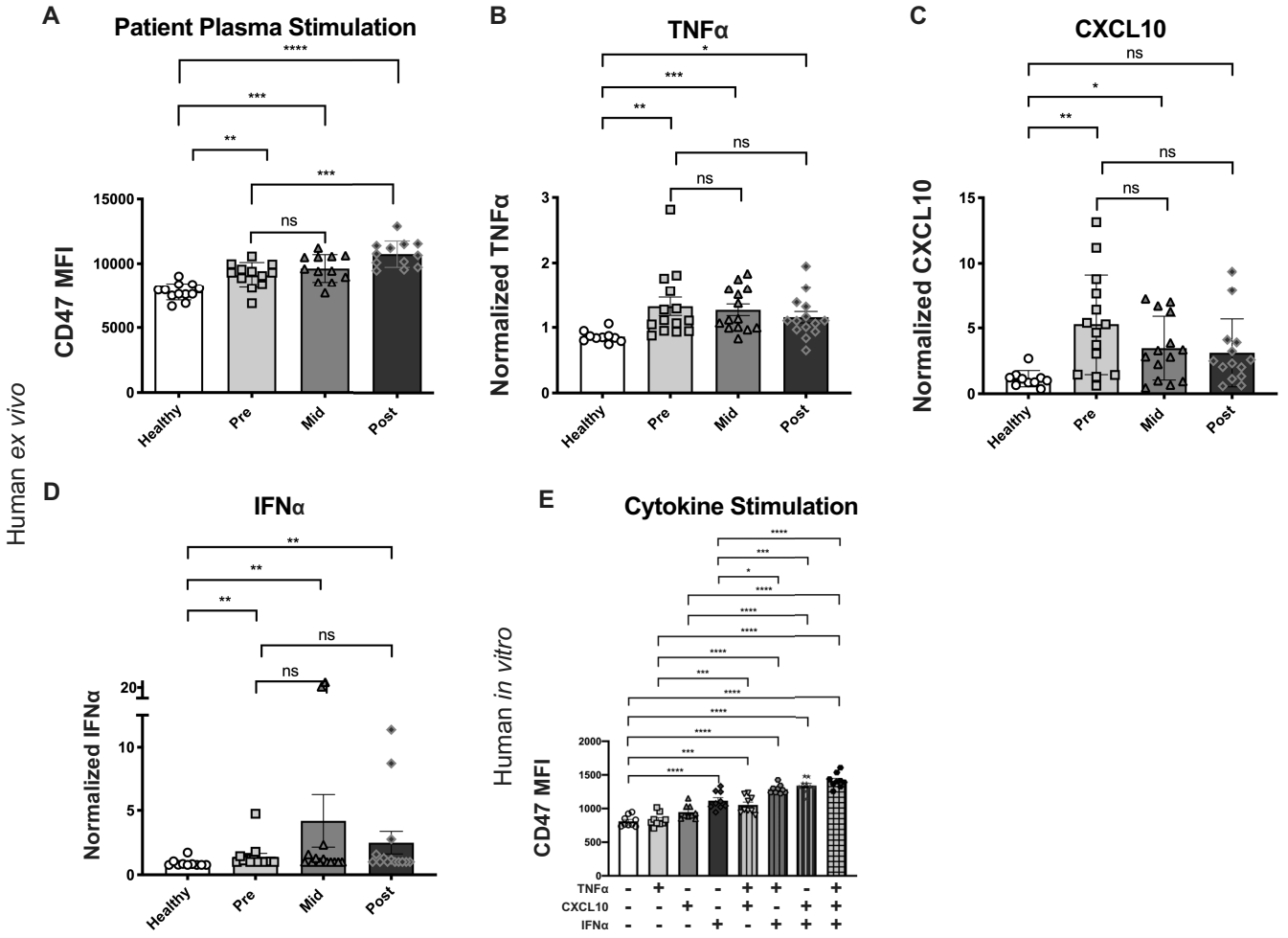

FIG 4 Plasma from HCV-infected patients is sufficient to increase CD47 expression on monocyte-derived DCs. (A) Quantitative comparison of CD47 CyTOF MFI of monocyte-derived DCs matured in culture medium containing plasma samples from the sofosbuvir HCV patient cohort before the initiation of treatment (Pre), midway through treatment (Mid), and after treatment (Post) compared to healthy controls. (B to D) Plasma collected from the sofosbuvir HCV patient cohort was analyzed by Luminex assays and normalized as described in Materials and Methods for TNF-α (B), CXCL10 (C), and IFN-α (D). (E) Comparison of CD47 MFI on HLA-DR$^+$ DCs 72 h after stimulation *in vitro* with 10 μg/ml TNF-α, 100 μg/ml CXCL10, and 100 μg/ml IFN-α as single treatments or in combination. Statistics were done by one-way ANOVA with multiple-comparison posttests (ns, $P > 0.05$; *, $P < 0.05$; **, $P < 0.01$; ***, $P < 0.001$; ****, $P < 0.0001$). Error bars represent SEM. Comparisons not labeled are not significantly different.

from blood samples of LCMV-infected mice at 8, 10, and 12 dpi in the presence or absence of CD47 blockade. At both 8 and 10 dpi, there were significantly increased CD8$^+$ T cell numbers responding to LCMV infection in the treated mice compared to the isotype-matched antibody control-treated mice (Fig. 5C).

Genetic inactivation of CD47 expression prolongs survival from *Mycobacterium tuberculosis* infection *in vivo*. We next investigated the role of CD47 during *Mycobacterium tuberculosis* infection *in vitro* and *in vivo*. First, human macrophages derived from healthy PBMC samples were used for *in vitro* infection with *M. tuberculosis* to examine CD47 expression levels. CD47 expression levels are shown for four donors, and compare naive macrophages from cultures that were not infected to macrophages from cultures that were infected with pHrodo-labeled *M. tuberculosis*. In comparison to naive macrophages, CD47 was not upregulated on *M. tuberculosis*-infected (pHrodo-positive [pHrodo$^+$]) macrophages (Fig. 5D). Interestingly, *M. tuberculosis*-uninfected (pHrodo-negative [pHrodo$^-$]) macrophages from the *M. tuberculosis*-infected cultures downregulated CD47 expression in comparison to naive macrophages, an observation for which we do not yet have an explanation (Fig. 5D). The lack of CD47 upregulation by *M. tuberculosis*-infected macrophages was supported by metasignature analysis

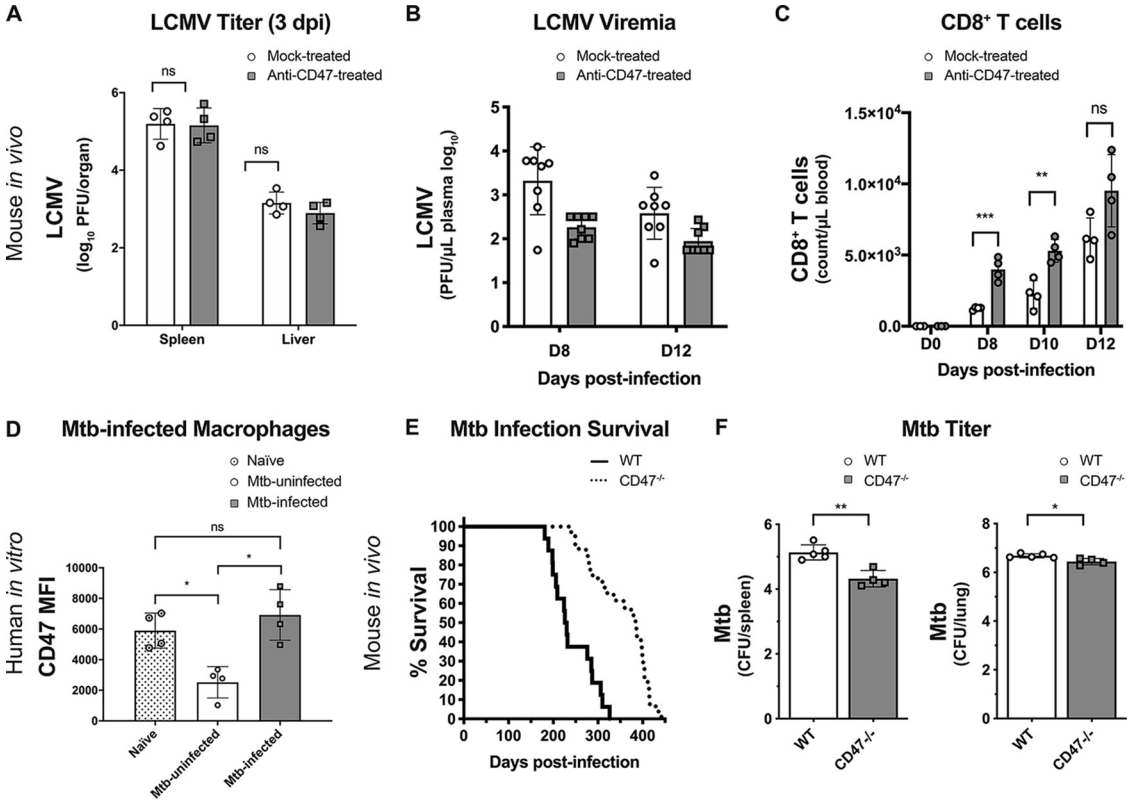

FIG 5 *In vivo* CD47 blockade in LCMV infection and CD47 genetic inactivation in *M. tuberculosis* infection. (A to C) Female C57BL/6 mice 8 to 12 weeks old were treated by intraperitoneal injection with either 100 μg anti-CD47 or an isotype control antibody at days -2, -1, 0, $+1$, and $+2$ relative to the day of intravenous infection (day 0 [D0]) with 2×10^6 PFU LCMV-WE. (A) Mice were euthanized at 3 dpi, and LCMV PFU from spleen and liver were determined as described in Materials and Methods. (B) LCMV viremia levels were determined from blood samples by plaque-forming assays for control and anti-CD47-treated mice at 8 and 12 dpi. (C) $CD8^+$ T cell counts in blood samples from control and anti-CD47-treated mice were analyzed by flow cytometry at 0, 8, 10, and 12 dpi. Statistics were done by unpaired two-way *t* tests (ns, $P > 0.05$; *, $P < 0.05$; **, $P < 0.01$; ***, $P < 0.001$). Error bars represent SEM. (D) Human peripheral blood monocyte-derived macrophages from four different donors were infected *in vitro* with *M. tuberculosis* (Mtb) (pantothenate/lysine mutant strain) fluorescently labeled with pHrodo (to distinguish infected from uninfected cells) in triplicate and stained with anti-CD47 at 24 h postinfection. Flow cytometry was used to measure CD47 MFI in cells from uninfected cultures (naive) compared to both infected and uninfected cells from *M. tuberculosis*-infected cultures. Statistics were done by one-way ANOVA with multiple-comparison posttests (ns, $P > 0.05$; *, $P < 0.05$). (E) Both male and female C57BL/6 WT ($n = 16$) and C57BL/6.CD47$^{-/-}$ ($n = 23$) mice were analyzed for survival (humane endpoints) following *M. tuberculosis* infection by inhalation. The difference between C57BL/6 WT and C57BL/6.CD47$^{-/-}$ mice was statistically significant (****, $P < 0.001$ by a log rank Mantel-Cox test from pooled data from three independent experiments). (F) Analysis of *M. tuberculosis* CFU from lungs and spleens of endpoint animals. Statistical analyses were done by Student's *t* tests, and two-sided *P* values are shown (*, $P < 0.05$; **, $P < 0.01$) with standard deviations.

comparing microarrays for gene expression signatures specific to HCV and tuberculosis (TB) (Fig. S2). The disease-specific gene expression signature for HCV consistently showed an upregulation of CD47, whereas the disease-specific gene expression signature for TB showed downregulation.

For an *in vivo* assessment of a possible functional role for CD47 in host resistance to *M. tuberculosis* infection, CD47 knockout (KO) mice were infected via the aerosol route with a low dose (100 to 200 CFU) of *M. tuberculosis* strain H37Rv. CD47-deficient mice displayed significantly increased host resistance to *M. tuberculosis* infection, with significantly longer survival (humane endpoints), compared to wild-type C57BL/6 mice (Fig. 5E). Furthermore, spleens and lungs from the CD47-deficient mice at humane endpoints yielded significantly lower mycobacterial CFU (Fig. 5F). These results indicated that CD47 expression can exert significant suppressive effects on immune responses to infectious pathogens *in vivo*.

DISCUSSION

Previous results demonstrating that malignant cells upregulate CD47 expression to evade cellular clearance (9, 31) led us to hypothesize that pathogens might also induce

CD47 surface expression as an immune evasion mechanism. In fact, poxviruses encode a CD47 mimic that acts as a potent virulence factor (20). Curiously, we repeatedly observed an upregulation of CD47 surface expression across diverse infections with both viruses and bacteria, none of which are known to encode a CD47 mimic or have any CD47 sequence homology. Flagella are potent inducers of TLRs, so the finding that *Salmonella* Typhi Δ*fliC* mutants lacking flagella were poor at inducing CD47 suggested a possible connection to host sensing via PRR signaling (Fig. 1F). Indeed, direct stimulation of PRRs with synthetic ligands such as MDP, CL264, and R848 induced CD47 upregulation *in vitro* and *in vivo* (Fig. 2). Since SIRPα-mediated recognition of CD47 on infected cells by macrophages and DCs transduces an inhibitory signal that attenuates phagocytosis and downstream antigen presentation functions, it was counterintuitive that CD47 upregulation would be due to a host response. Why would the host dampen its immune response to infection? We have shown that *in vivo*, CD47 blockade improved the control of LCMV infection (Fig. 5A), increased $CD8^+$ T cell responses (Fig. 5C), and, in a previous report, increased the expression of costimulatory molecules on APCs as well (23), thus confirming that CD47 induces immunosuppressive signals. Similarly, mice with genetic inactivation of CD47 had reduced bacterial loads and longer survival times when infected with *M. tuberculosis* (Fig. 5E and F). We conclude that, like coinhibitory molecules such as PD-1 that dampen adaptive immune responses, CD47 upregulation acts as an intrinsic governor of the innate immune response to prevent overactivation that can lead to immunopathology. Thus, the initial immune response to infections is attenuated until proinflammatory signals overcome anti-inflammatory signals.

CD47 was previously identified by microarray analysis as an interferon-stimulated gene (ISG), upregulated as part of a coordinated program of host defense mechanisms upon IFN-α stimulation (32). In addition, TNF-α was demonstrated to induce the upregulation of CD47 on vascular smooth muscle cells *in vitro* (33). In breast cancer, TNF-α-mediated CD47 upregulation is transcriptionally controlled by NF-κB through an NF-κB motif within an enhancer of the CD47 gene (34). These reports are consistent with our findings showing that the inflammatory milieu in patient blood during HCV infection is sufficient to upregulate CD47 surface expression (Fig. 4E). While our study focused on TNF-α, CXCL10, and IFN-α, redundant mechanisms of CD47 upregulation by additional inflammatory mediators are possible and should be examined in depth in future experiments. In the experimental models utilized, it is difficult to distinguish the relative contributions of cytokine-induced CD47 upregulation from those of direct pathogen-induced CD47 upregulation where both are present and either is sufficient. The results clearly indicate that CD47 surface expression can be upregulated either in a cell-intrinsic manner via stimulation of PRRs or by surveilling immune cells in response to extrinsic signaling by inflammatory cytokines. It may also be possible that signaling via *cis* interactions within a cell could occur in cells such as macrophages, which express both CD47 and SIRPα.

Of the infectious agents that we analyzed, *M. tuberculosis* infection was unique in failing to induce CD47 expression upon infection. Of interest, uninfected cells from *M. tuberculosis*-infected cultures downregulated CD47 expression. This may not be too surprising because the life cycle of *M. tuberculosis* is dependent on phagocytosis by alveolar macrophages, and *M. tuberculosis* is known to induce strong inflammatory responses via the induction of cytokines and chemokines. Further research will be required to identify the mechanisms involved in these unique responses to *M. tuberculosis*, but despite its failure to upregulate CD47, improved survival from *M. tuberculosis* infection was observed in mice genetically deficient in CD47 compared to wild-type mice (Fig. 5E). Better recoveries from malaria parasites (35, 36) and *Escherichia coli* infections (37) have also been shown in CD47 KO mice. In addition, CD47 KO mice have improved influenza virus vaccine responses (16). However, from an evolutionary standpoint, the upregulation of CD47 expression in response to pathogens must result in a competitive advantage for the host. As an example, CD47 KO mice show poorly controlled inflammatory responses to and increased morbidity and mortality from

Candida albicans infection (38). The contrasting results from various infections in CD47 KO mice illustrate how tightly balanced the immune system has evolved to be and the care that must be taken when immune interventions are undertaken. That said, the results from CD47 KO mice, in which the entire immune system has developed in the absence of a critical immunomodulatory molecule, might produce different results than the same infection in an immune-replete mouse treated with anti-CD47 antibodies during the infectious process. Indeed, while we found that treating wild-type mice with anti-CD47 before LCMV strain WE (LCMV-WE) infection improved recovery, it has been reported that CD47 KO mice have decreased resistance to LCMV Clone-13 infections (39). Additional experiments will be required to determine which experimental factors may account for the differences in these outcomes.

The accelerated $CD8^+$ T cell responses and clearance of LCMV infections following prophylactic blockade of CD47 were most likely due to enhanced APC function evidenced by the increased expression of costimulatory CD86 on dendritic cells observed at 3 dpi (23). However, it is also possible that there were direct effects on $CD8^+$ T cells since it was previously shown that activated $CD8^+$ T cells express SIRPα, the receptor for CD47 (17). It was shown that only activated effector cells and not naive $CD8^+$ T cells express SIRPα, and any direct effects on $CD8^+$ T cells would occur only after expansion and development of effector functions. Furthermore, in contrast to the negative signal delivered to cells of the monocytic lineage via SIRPα ligation to CD47, evidence suggested that CD47-SIRPα signaling in $CD8^+$ T cells delivered a positive signal associated with improved cytolytic killing of infected target cells *in vivo*. The $CD8^+$ T cell responses measured in this prophylactic anti-CD47 study were total $CD8^+$ T cell responses rather than tetramer-stained cells known to be virus specific. Thus, the expansion of bystander $CD8^+$ T cells by anti-CD47 was not excluded. However, when anti-CD47 was used in a therapeutic setting against LCMV infections, the predominant $CD8^+$ T cell expansions were virus specific, and the mechanism of protection was dependent on DCs and $CD8^+$ T cells (23).

The current results demonstrate that CD47 plays a prominent role in modulating inflammatory responses to infections. While these findings open new possibilities for therapeutic intervention against pathogenic agents, it is important to note that the context of the host response to specific types of infections will determine whether CD47 blockade would be protective or detrimental. There may be circumstances where host responses need boosting, and CD47 represents a novel target for host-directed therapies in such cases. Possibilities include viruses such as SARS-CoV-2, human immunodeficiency virus, human papillomavirus, cytomegalovirus, Epstein-Barr virus, varicella-zoster virus, and Ebola virus, etc. There is also a potential application for treating infections with bacteria, including *M. tuberculosis* and multidrug-resistant bacterial strains that might otherwise be untreatable. Although not addressed in this study, other infectious agents, such as fungi or parasites, that elicit PRR responses might also be tractable to anti-CD47 therapy. A key factor is that infected cells also express damage-associated molecular patterns (DAMPs), which act as "eat me" signals that are being masked by the CD47 "don't eat me" signal (11, 40). Therefore, releasing the inhibition of phagocytosis of these cells would need to be weighed cautiously with the extent of infection and the replaceability of the infected cell types.

MATERIALS AND METHODS

All animal studies were performed at NIAID Laboratories and Stanford University and were done so under animal study proposals approved by the Institutional Animal Care and Use Committees following all regulations and guidelines of the Public Health Service's Office of Laboratory Animal Welfare.

Murine *in vivo* viral infections and flow cytometry analysis. Friend virus (FV)-infected mice were female (C57BL/10 × A.BY)F_1 (abbreviated Y10) (H-$2^{b/b}$, Fv1^b, Rfv$3^{r/s}$) mice bred at the Rocky Mountain Laboratories (RML) (Hamilton, MT) and were used at between 8 and 16 weeks of age at the beginning of the experiments. The FV stock used in these experiments has been passaged in mice for more than 3 decades and contains three separate viruses: (i) replication-competent B-tropic Friend murine leukemia helper virus (F-MuLV), (ii) replication-defective polycythemia-inducing spleen focus-forming retrovirus that is packaged by F-MuLV-encoded virus particles, and (iii) lactate dehydrogenase-elevating virus (LDV), an endemic murine positive-sense ssRNA [(+)ssRNA] virus (22, 41). Mice were infected by intravenous

(i.v.) injection of 0.2 ml of a phosphate-buffered balanced salt solution (PBS) containing 1,500 spleen focus-forming units (SFFU) of the FV complex. La Crosse virus (LACV) infections were performed with a 1978 human isolate provided as a gift from Stephen Whitehead (NIAID, NIH). Virus stocks were passaged no more than 3 times in Vero cells. For analysis of CD47 expression in mice during LACV infection, 21-day-old C57BL/6 (Jackson Laboratories) male or female mice were inoculated intraperitoneally with a 10^5-PFU dose of virus diluted into a 200-μl volume of sterile PBS. Mice of the same strain, age, and sex inoculated with an equivalent volume of a Vero cell culture supernatant in PBS were used as controls. At 2 dpi, whole blood and spleen were isolated from mice and processed for flow cytometry as described above. LCMV viral titers were detected by plaque-forming assays on MC57 fibroblasts (obtained from by the Ontario Cancer Institute, Canada). Organs were dissociated, and plasma was diluted in Dulbecco's modified Eagle medium (DMEM) containing 2% fetal calf serum (FCS), titrated 1:3 over 12 steps, and incubated on MC57 cells. After 4 h of incubation at 37°C, a methylcellulose overlay was added, and the cells were incubated for 48 h, followed by staining of LCMV plaques using an anti-LCMV-NP antibody (clone VL4). C57BL/6 mice were infected with 2×10^6 PFU of LCMV strain WE and treated with anti-CD47 via daily intraperitoneal injections of 100 μg of anti-CD47 (clone 410, catalog number BE0283; BioXCell) or an isotype control (rat IgG2a isotype) (BioXCell) from day −2 to day 6 postinfection.

To analyze infected spleen cells, splenocytes were isolated by tissue homogenization through a 100-μm filter, and red blood cells were removed using ACK lysis buffer (0.15 M NH_4Cl, 10 mM $KHCO_3$, 0.1 M EDTA). The gating strategy for spleen cell subset analyses was the same as the one described previously (23). All antibodies were from BD Biosciences, BioLegend, or eBioscience/Thermo Fisher Scientific, including Brilliant Violet 605-anti-CD11b (clone M1/70), phycoerythrin (PE)-CF594-anti-CD19 (clone ID3), PE-Cy7-anti-CD11c (clone HL3), PE-Cy7-anti-Ter119 (clone TER-119), Alexa Fluor 647-anti-CD47 (clone MIAP301), and fluorescein isothiocyanate (FITC)-anti-major histocompatibility complex class II (MHCII) (I-A/I-E) (catalog number FAB6118F); lymphocyte populations were initially gated on single live cells on the basis of forward scatter (FSC) versus side scatter (SSC). Mouse DCs were defined as $CD11c^+$ $CD11b^-$, and macrophages were defined as $CD11c^-$ $CD11b^+$. Human DCs were also gated on the basis of high MHCII expression levels. The $CD11c^+$ subset contained a minor population of CD11b-intermediate cells that could have been inflammatory macrophages. The multiparameter data were collected with an LSRII instrument (BD Biosciences) and analyzed using FlowJo software.

Bacterial strains. Bacterial strains included a B31 *Borrelia burgdorferi* clone (GCB726) with the cp9 plasmid replaced by a cp9-based pTM61 construct containing green fluorescent protein (GFP) (42). *Salmonella enterica* serovar Typhi Ty2 mCherry mutant strains were generated via λ red recombination and included the *Salmonella enterica* serovar Typhi Ty2 mCherry ΔFla (*fliC*::Kan) mutant (25). *M. tuberculosis* H37Rv Δ*lysA* and Δ*panCD*, used for the *in vitro* studies, were provided by William R. Jacobs, Jr. (43). *M. tuberculosis* strain H37Rv was used for the *in vivo* studies.

Affymetrix array profiles of liver biopsy specimens. Affymetrix arrays were obtained as CEL files, MAS5 normalized using the "affy" package in Bioconductor, mapped to NCBI Entrez gene identifiers using a custom chip definition file (Brainarray version 19 [http://brainarray.mbni.med.umich.edu/Brainarray/]), and converted to HUGO gene symbols (44).

SARS-CoV-2. A publicly available gene expression data set from SARS-CoV-2 infection of A549 cells (accession number GSE147507) ($n = 10$) was downloaded from the Gene Expression Omnibus (GEO). Independent biological replicates of transformed lung alveolar (A549) cells were mock infected (uninfected [Un]) ($n = 13$) or infected (Inf) ($n = 6$) with SARS-CoV-2 (USA-WA1/2020). cDNA libraries were sequenced from each sample using the Illumina NextSeq 500 platform. Raw sequencing reads were aligned to the human genome (hg19) using the RNA-Seq Alignment App (v2.0.1) on Basespace (Illumina, CA). Gene expression values were summarized using counts per million (CPM) and converted to a $\log_2$ scale using the formulas $\log_2$(CPM) if the CPM were >1 and CPM − 1 if the CPM were <1. A standard *t* test was performed using the Python scipy.stats.ttest_ind package (version 0.19.0) with Welch's two-sample *t* test (unpaired, unequal variance [equal_var=False], and unequal sample size) parameters. The results were independently validated with R statistical software (R version 3.6.1, 5 July 2019). CD47 was significantly upregulated ($P = 0.00332$) in SARS-CoV-2-infected samples. (45).

HCV sofosbuvir cohort. PBMCs, plasma, and serum were studied in 14 HCV-infected patients previous to direct-acting antiviral therapy (sofosbuvir [SOF] and simeprevir [SIM]; SOF and ribavirin [RBV]; and SOF, RBV, and pegylated interferon [PEG]) before treatment, during treatment, and after treatment. Ten patients underwent at least one previous treatment with interferon, and the other four were treatment naive. Thirteen patients experienced a sustained virologic response (SVR) after 12 weeks of therapy. PBMCs, plasma, and serum were collected from noninfected patients as a control (Table 1). One patient relapsed. Patients provided written informed consent for research testing under protocols by the Stanford University Institutional Review Board.

Phospho-CyTOF sample processing and staining. Cryopreserved PBMCs stored at −180°C were thawed in warm RPMI medium supplemented with 10% FBS, Benzonase, and a penicillin-streptomycin mixture (complete RPMI medium). Cells were transferred into serum-free RPMI medium containing 2 mM EDTA and Benzonase, incubated with cisplatin for 1 min, and immediately quenched with 4 volumes of complete RPMI medium. Next, 1 million cells per sample were transferred into complete RPMI medium and rested for 30 min at 37°C. Following this rest period, cells were fixed in PBS with 2% paraformaldehyde (PFA) at room temperature for 10 min. Cells were then washed twice with CyFACS buffer and barcoded as previously described (46). Following barcoding, samples were combined for surface marker staining, performed at room temperature for 1 h. Subsequently, cells were washed and permeabilized in methanol (MeOH) at −80°C overnight. The next day, cells were washed and incubated with the intracellular cytokine cocktail at room temperature for 1 h. DNA staining was performed for 20 min with

TABLE 1 HCV sofosbuvir cohort

Patient	Previous IFN	Genotype	Treatments	Liver transplant waitlist	Outcome	Sex	Viral titer (copies/ml)
2	Yes	1	SOF, SIM	No	SVR	Male	1,790,000
4	Yes	1	SOF, SIM	No	SVR	Female	921,000
7	No	2	SOF, RBV	No	SVR	Female	2,180,000
8	Yes	2	SOF, RBV	No	SVR	Female	5,380,000
9	Yes	1	SOF, SIM	No	SVR	Male	2,230,000
12	No	2	SOF, RBV	No	SVR	Female	3,160,000
13	No	1	SOF, SIM	Yes	Relapse	Female	696,000
14	Yes	1	SOF, SIM	No	SVR	Male	9,290,000
20	Yes	1	SOF, SIM	No	SVR	Male	50,000,000
22	Yes	1	SOF, PEG, RBV	No	SVR	Female	5,030,000
27	Yes	1	SOF, SIM	No	SVR	Male	148,505
29	Yes	1	SOF, SIM	Yes	SVR	Male	2,630,000
30	No	4	SOF, PEG, RBV	No	SVR	Female	1,200,000
35	No	1	SOF, SIM	No	SVR	Male	79,900
38	Yes	1	SOF, SIM	No	SVR	Male	6,556,280

iridium (191/193) in PBS with 2% PFA at room temperature. Finally, cells were washed twice with CyFACS buffer and then twice with MilliQ water before data acquisition on the CyTOF2 instrument. Data were debarcoded and manually analyzed on Cytobank (www.cytobank.org/).

Monocyte-derived DC and macrophage cultures. Healthy donor leukocyte reduction system cones were provided by the Stanford blood center. PBMCs were isolated by a 1.077-g/ml Ficoll gradient using Sep-mate tubes. Monocytes were selected for by plastic adherence after 20 min of incubation at 37°C with 5% CO_2 in RPMI medium plus 10% human serum (Gemini). Selected monocytes were then cultured for 72 h in RPMI medium supplemented with 1% serum, 10 ng/ml interleukin-4 (IL-4), and 800 IU/ml granulocyte-macrophage colony-stimulating factor (GM-CSF); the concentration of GM-CSF was increased to 1,600 IU/ml for the final 24 h. Immature DCs were matured by replacing culture medium with RPMI medium supplemented with 1% healthy donor or HCV patient plasma, 10 ng/ml IL-4, 800 IU/ml GM-CSF, 10 mg/ml lipopolysaccharide (LPS), and 100 IU/ml IFN-γ. For macrophage derivation, monocytes were cultured in RPMI medium supplemented with 10% human serum for 7 days.

Human and murine Luminex assays. The human samples were analyzed at the Human Immune Monitoring Center at Stanford University. Human 63-plex or mouse 38-plex kits were purchased from eBioscience/Affymetrix and used according to the manufacturer's recommendations, with modifications as described below. Briefly, beads were added to a 96-well plate and washed in a BioTek ELx405 washer. Samples were added to the plate containing mixed antibody-linked beads and incubated at room temperature for 1 h, followed by incubation overnight at 4°C with shaking. Cold and room-temperature incubation steps were performed on an orbital shaker at 500 to 600 rpm. Following incubation overnight, plates were again washed in a BioTek ELx405 washer, and a biotinylated detection antibody was then added for 75 min at room temperature, with shaking. The plate was washed as described above, and streptavidin-PE was added. After incubation for 30 min at room temperature, another wash was performed as described above, and reading buffer was added to the wells. Each sample was measured in duplicate. Plates were read using a Luminex 200 instrument with a lower bound of 50 beads per sample per cytokine. Custom assay control beads by Radix Biosolutions were added to all wells.

***In vitro* stimulations and infections of human PBMCs and macrophages.** Healthy donor leukocyte reduction system cones were provided by the Stanford blood center. Human PBMCs were isolated by a 1.077-g/ml Ficoll gradient using Sep-mate tubes. Isolated PBMCs were cultured in RPMI medium supplemented with 10% FBS and 100 U/ml penicillin-streptomycin at a concentration of 1×10^6 cells/ml. To activate PRRs, cells were stimulated with either 1 μg/ml CL264-rhodamine (InvivoGen), 1 μg/ml muramyl dipeptide (InvivoGen), or R848 at concentrations of 0.1 μg/ml, 1 μg/ml, and 10 μg/ml or left unstimulated. Cells were collected at 48 h poststimulation prior to flow cytometry. PBMCs were stimulated with single treatments or combination treatments of 10 ng/ml TNF-α, 100 ng/ml CXCL10, and 100 ng/ml IFN-α. Cells were then analyzed for CD47 expression 72 h after cytokine stimulation. *In vitro* bacterial infections of PBMCs were performed at a multiplicity of infection (MOI) of 10 for *Salmonella enterica* serovar Typhi strains and at an MOI of 40 for *Borrelia burgdorferi*, for 24 and 48 h, respectively. *Salmonella enterica* serovar Typhi strains were spun onto the cells to compensate for the motility differences. Indeed, the strain of *Salmonella enterica* serovar Typhi infected a lower percentage of cells, but infected versus uninfected cells were differentiated for the analyses. For *M. tuberculosis in vitro* infection of macrophages, *M. tuberculosis* was stained for 1 h in PBS with a 1:20,000 dilution of pHrodo (Essen Biosciences) at 37°C to fluorescently label infected macrophages. Macrophages were plated into 96-well U-bottom plates. Fluorescently labeled *M. tuberculosis* bacteria were used to infect macrophages at an MOI of 1:10 for 24 h. For antibodies for flow cytometry, anti-CD11c (clone 3.9), anti-HLA-DR (clone L243), anti-CD11b (clone M1/70), anti-CD14 (clone M5E2), anti-CD16 (clone 3G8), and anti-SIRP (clone SE5A5) were purchased from BioLegend, except for allophycocyanin (APC)-anti-CD47 (clone B6H12; eBioscience), which was purchased from Invitrogen. Cells were analyzed with 4′,6-diamidino-2-phenylindole (DAPI) for dead-cell exclusion and then gated on single cells using FSC-a (forward scatter

area) by FSC-h (forward scatter height) and SSC-a (side scatter area) by SSC-h (side scatter height). Dendritic cells were defined as MHCII/HLA-DR^{hi} and CD11c^{hi}.

All human *in vitro* experiments were repeated in at least two independent experiments with a minimum of 4 biological replicates.

***In vivo* and *in vitro* stimulation of mouse cells.** Female C57BL/6 RRID:IMSR_JAX:000664 (WT) mice were bred at the Stanford University Stem Cell Institute Barrier Facility (Stanford, CA) and used at between 8 and 12 weeks of age at the beginning of the experiments. For R848 *in vivo* analysis, 10 naive mice were injected intraperitoneally with either 1 mg/kg of body weight of R848 or PBS, all at a volume of 0.1 ml, for three consecutive days. On day 3 after the first treatment, splenocytes were isolated. Spleens were dissociated by collagenase treatment in the presence of DNase I and mechanical dissociation to obtain a single-cell suspension of splenocytes. Red blood cells were removed using ACK lysis buffer (Gibco), and the remaining splenocytes were seeded at a density of 1×10^6 splenocytes/well in a 96-well U-bottom low-adherence plate. Cells were then stained for the macrophage and DC markers CD11b, MHCII, and CD11c, as well as SIRPα and CD47, with DAPI for live/dead exclusion. For *in vitro* stimulation, splenocytes were isolated from naive mice as described above and then stimulated with either 1 μg/ml CL264-rhodamine (InvivoGen) overnight or 1 μg/ml poly(I·C)-rhodamine (InvivoGen) complexed with Lipofectamine 2000 for 1 h or left unstimulated. Cells were collected at 24 h poststimulation for analysis by flow cytometry. Antibodies for flow cytometry were purchased from BioLegend or BD Biosciences.

***M. tuberculosis* infections.** *M. tuberculosis* infections were done in C57BL/6 mice or CD47 KO RRID:IMSR_JAX:003173 (CD47 KO) mice that were bred at NIAID facilities. For infections with *M. tuberculosis* H37Rv (100 to 200 CFU), 8- to 12-week-old male and female mice were placed in a whole-body inhalation system (Glas-Col, Terre Haute, IN) and exposed to aerosolized *M. tuberculosis*. Delivery doses were set by measuring lung CFU at 2 to 24 h postexposure from three to five control mice through mechanical homogenization using Precellys Evolution (Precellys, Atkinson, NH). Lung homogenates were then serially diluted in PBS-Tween 20 and cultured on Middlebrook 7H11 agar plates supplemented with oleic acid-albumin-dextrose-catalase (Difco, Detroit, MI), and CFU were counted 21 days later.

Cell isolation from *M. tuberculosis*-infected lung tissue and flow cytometry. Lungs were digested and dissociated using gentle magnetically activated cell sorting (MACS) and lung cell isolation buffer (Miltenyi Biotec). The digested lung was passed through a 100-mm cell strainer, and an aliquot was removed for the determination of CFU. Cells were washed and purified with 37% Percoll. Cells for sorting were washed, counted, and subsequently surface stained in a biosafety level 3 (BSL3) containment area under sterile conditions. The following cell populations were sorted to 90 to 97% purity and plated for CFU counts: CD45.1$^+$ (WT) or CD45.1$^-$ (Il1r12/2) CD11b$^+$, CD11b$^+$ Gr1^{high} (neutrophils), and CD11b$^+$ Gr1^{low} (myeloid). Abs against I-Ab (clone M5/114.15.2), Ly6G (clone 1A8), CD11c (clones HL3 and N418), CD45.1 (clone A20), CD45.2 (clone 104), T cell receptor β (TCRβ) (clone H57-597), NK1.1 (clone PK136), CD11b (clone M1/70), CD45 (clone 30-F11), and Gr-1 (clones RB6 and 8C5) and live/dead fixable cell stains were obtained from eBioscience/Thermo Fisher Scientific, BioLegend, or BD Pharmingen. Samples were acquired on a 350 Symphony flow cytometer or sorted on a FACSAria instrument (BD Biosciences, San Jose, CA) and analyzed using FlowJo software.

SUPPLEMENTAL MATERIAL

Supplemental material is available online only.

FIG S1, PDF file, 0.5 MB.

FIG S2, PDF file, 0.4 MB.

ACKNOWLEDGMENTS

We thank members of the Weissman, Hasenkrug, Davis, and Glenn laboratories, especially Da Yoon No and Nathaniel Fernhoff, for helpful advice, discussions, and reagents. We specifically acknowledge Aaron Newman for assistance and guidance in the analysis of microarray data. We thank Susan Matlock Brewer for assistance and guidance with salmonella experiments. We thank Yael Rosenberg-Hasson and the staff of the Stanford Human Immune Monitoring Center for their technical expertise and for running the mouse and human Luminex assays. We also acknowledge the laboratory of Benjamin R. tenOever and Daniel Blanco-Melo for the rapid sharing of critical SARS-CoV-2 data at the onset of this pandemic (GEO accession number GSE147507).

Research reported in this publication was supported by the Intramural Research Program of the National Institute of Allergy and Infectious Diseases, National Institutes of Health; the Virginia and D. K. Ludwig Fund for Cancer Research; the Robert J. Kleberg, Jr., and Helen C. Kleberg Foundation; AML grant R01CA086017; the PCBC from NIHLB U01HL099999; as well as grant U19AI109662. M.C.T. and Y.Y.Y. were supported by Stanford Immunology training grant 5T32AI007290, and M.C.T. was also supported by the NIH NRSA 1 F32 AI124558-01 award and the Bay Area Lyme Foundation. L.B.T.D. was supported by a Stanford Diversifying Academia Recruiting Excellence fellowship. E.P.

was supported by grant F30DK099017 and the Stanford Medical Scientist Training Program. The funders had no role in study design, data collection and analysis, decision to publish, or preparation of the manuscript.

K.J.H. and I.L.W. are listed as inventors on U.S. patent 2019/0092873 A1 CD47, Targeted Therapies for the Treatment of Infectious Disease. I.L.W. is a cofounder, director, and stockholder in Forty Seven Inc., a public company that was involved in CD47-based immunotherapy of cancer during this study but was acquired by Gilead. At the time of this submission, I.L.W. has no formal relationship with Gilead.

REFERENCES

1. Barber DL, Wherry EJ, Masopust D, Zhu B, Allison JP, Sharpe AH, Freeman GJ, Ahmed R. 2006. Restoring function in exhausted CD8 T cells during chronic viral infection. Nature 439:682–687. https://doi.org/10.1038/nature04444.
2. Dyck L, Mills KHG. 2017. Immune checkpoints and their inhibition in cancer and infectious diseases. Eur J Immunol 47:765–779. https://doi.org/10.1002/eji.201646875.
3. Wei SC, Anang N-AAS, Sharma R, Andrews MC, Reuben A, Levine JH, Cogdill AP, Mancuso JJ, Wargo JA, Pe'er D, Allison JP. 2019. Combination anti-CTLA-4 plus anti-PD-1 checkpoint blockade utilizes cellular mechanisms partially distinct from monotherapies. Proc Natl Acad Sci U S A 116:22699–22709. https://doi.org/10.1073/pnas.1821218116.
4. Advani R, Flinn I, Popplewell L, Forero A, Bartlett NL, Ghosh N, Kline J, Roschewski M, LaCasce A, Collins GP, Tran T, Lynn J, Chen JY, Volkmer J-P, Agoram B, Huang J, Majeti R, Weissman IL, Takimoto CH, Chao MP, Smith SM. 2018. CD47 blockade by Hu5F9-G4 and rituximab in non-Hodgkin's lymphoma. N Engl J Med 379:1711–1721. https://doi.org/10.1056/NEJMoa1807315.
5. Sikic BI, Lakhani N, Patnaik A, Shah SA, Chandana SR, Rasco D, Colevas AD, O'Rourke T, Narayanan S, Papadopoulos K, Fisher GA, Villalobos V, Prohaska SS, Howard M, Beeram M, Chao MP, Agoram B, Chen JY, Huang J, Axt M, Liu J, Volkmer J-P, Majeti R, Weissman IL, Takimoto CH, Supan D, Wakelee HA, Aoki R, Pegram MD, Padda SK. 2019. First-in-human, first-in-class phase I trial of the anti-CD47 antibody Hu5F9-G4 in patients with advanced cancers. J Clin Oncol 37:946–953. https://doi.org/10.1200/JCO.18.02018.
6. Takimoto CH, Chao MP, Gibbs C, McCamish MA, Liu J, Chen JY, Majeti R, Weissman IL. 2019. The macrophage 'do not eat me' signal, CD47, is a clinically validated cancer immunotherapy target. Ann Oncol 30:486–489. https://doi.org/10.1093/annonc/mdz006.
7. Chao MP, Takimoto CH, Feng DD, McKenna K, Gip P, Liu J, Volkmer J-P, Weissman IL, Majeti R. 2020. Therapeutic targeting of the macrophage immune checkpoint CD47 in myeloid malignancies. Front Oncol 9:1380. https://doi.org/10.3389/fonc.2019.01380.
8. Willingham SB, Volkmer J-P, Gentles AJ, Sahoo D, Dalerba P, Mitra SS, Wang J, Contreras-Trujillo H, Martin R, Cohen JD, Lovelace P, Scheeren FA, Chao MP, Weiskopf K, Tang C, Volkmer AK, Naik TJ, Storm TA, Mosley AR, Edris B, Schmid SM, Sun CK, Chua M-S, Murillo O, Rajendran P, Cha AC, Chin RK, Kim D, Adorno M, Raveh T, Tseng D, Jaiswal S, Enger PO, Steinberg GK, Li G, So SK, Majeti R, Harsh GR, van de Rijn M, Teng NNH, Sunwoo JB, Alizadeh AA, Clarke MF, Weissman IL. 2012. The CD47-signal regulatory protein alpha (SIRPa) interaction is a therapeutic target for human solid tumors. Proc Natl Acad Sci U S A 109:6662–6667. https://doi.org/10.1073/pnas.1121623109.
9. Jaiswal S, Jamieson CHM, Pang WW, Park CY, Chao MP, Majeti R, Traver D, van Rooijen N, Weissman IL. 2009. CD47 is upregulated on circulating hematopoietic stem cells and leukemia cells to avoid phagocytosis. Cell 138:271–285. https://doi.org/10.1016/j.cell.2009.05.046.
10. Majeti R, Becker MW, Tian Q, Lee T-LM, Yan X, Liu R, Chiang J-H, Hood L, Clarke MF, Weissman IL. 2009. Dysregulated gene expression networks in human acute myelogenous leukemia stem cells. Proc Natl Acad Sci U S A 106:3396–3401. https://doi.org/10.1073/pnas.0900089106.
11. Chao MP, Jaiswal S, Weissman-Tsukamoto R, Alizadeh AA, Gentles AJ, Volkmer J, Weiskopf K, Willingham SB, Raveh T, Park CY, Majeti R, Weissman IL. 2010. Calreticulin is the dominant pro-phagocytic signal on multiple human cancers and is counterbalanced by CD47. Sci Transl Med 2:63ra94. https://doi.org/10.1126/scitranslmed.3001375.
12. Gao A-G, Lindberg FP, Finn MB, Blystone SD, Brown EJ, Frazier WA. 1996. Integrin-associated protein is a receptor for the C-terminal domain of thrombospondin. J Biol Chem 271:21–24. https://doi.org/10.1074/jbc.271.1.21.
13. Jiang P, Lagenaur CF, Narayanan V. 1999. Integrin-associated protein is a ligand for the P84 neural adhesion molecule. J Biol Chem 274:559–562. https://doi.org/10.1074/jbc.274.2.559.
14. Brown EJ, Frazier WA. 2001. Integrin-associated protein (CD47) and its ligands. Trends Cell Biol 11:130–135. https://doi.org/10.1016/s0962-8924(00)01906-1.
15. Barclay AN, van den Berg TK. 2014. The interaction between signal regulatory protein alpha (SIRPα) and CD47: structure, function, and therapeutic target. Annu Rev Immunol 32:25–50. https://doi.org/10.1146/annurev-immunol-032713-120142.
16. Lee Y-T, Ko E-J, Lee Y, Lee Y-N, Bian Z, Liu Y, Kang S-M. 2016. CD47 plays a role as a negative regulator in inducing protective immune responses to vaccination against influenza virus. J Virol 90:6746–6758. https://doi.org/10.1128/JVI.00605-16.
17. Myers LM, Tal MC, Torrez Dulgeroff LB, Carmody AB, Messer RJ, Gulati G, Yiu YY, Staron MM, Angel CL, Sinha R, Markovic M, Pham EA, Fram B, Ahmed A, Newman AM, Glenn JS, Davis MM, Kaech SM, Weissman IL, Hasenkrug KJ. 2019. A functional subset of CD8+ T cells during chronic exhaustion is defined by SIRPα expression. Nat Commun 10:794. https://doi.org/10.1038/s41467-019-08637-9.
18. Legrand N, Huntington ND, Nagasawa M, Bakker AQ, Schotte R, Strick-Marchand H, de Geus SJ, Pouw SM, Böhne M, Voordouw A, Weijer K, Di Santo JP, Spits H. 2011. Functional CD47/signal regulatory protein alpha (SIRP(alpha)) interaction is required for optimal human T- and natural killer- (NK) cell homeostasis in vivo. Proc Natl Acad Sci U S A 108:13224–13229. https://doi.org/10.1073/pnas.1101398108.
19. Taylor KE, Mossman KL. 2013. Recent advances in understanding viral evasion of type I interferon. Immunology 138:190–197. https://doi.org/10.1111/imm.12038.
20. Cameron CM, Barrett JW, Mann M, Lucas A, McFadden G. 2005. Myxoma virus M128L is expressed as a cell surface CD47-like virulence factor that contributes to the downregulation of macrophage activation in vivo. Virology 337:55–67. https://doi.org/10.1016/j.virol.2005.03.037.
21. Dittmer U, Sutter K, Kassiotis G, Zelinskyy G, Bánki Z, Stoiber H, Santiago ML, Hasenkrug KJ. 2019. Friend retrovirus studies reveal complex interactions between intrinsic, innate and adaptive immunity. FEMS Microbiol Rev 43:435–456. https://doi.org/10.1093/femsre/fuz012.
22. Robertson SJ, Ammann CG, Messer RJ, Carmody AB, Myers L, Dittmer U, Nair S, Gerlach N, Evans LH, Cafruny WA, Hasenkrug KJ. 2008. Suppression of acute anti-Friend virus CD8+ T-cell responses by coinfection with lactate dehydrogenase-elevating virus. J Virol 82:408–418. https://doi.org/10.1128/JVI.01413-07.
23. Cham LB, Torrez Dulgeroff LB, Tal MC, Adomati T, Li F, Bhat H, Huang A, Lang PA, Moreno ME, Rivera JM, Galkina SA, Kosikova G, Stoddart CA, McCune JM, Myers LM, Weissman IL, Lang KS, Hasenkrug KJ. 2020. Immunotherapeutic blockade of CD47 inhibitory signaling enhances innate and adaptive immune responses to viral infection. Cell Rep 31:107494. https://doi.org/10.1016/j.celrep.2020.03.058.
24. Hayashi F, Means TK, Luster AD. 2003. Toll-like receptors stimulate human neutrophil function. Blood 102:2660–2669. https://doi.org/10.1182/blood-2003-04-1078.
25. Kortmann J, Brubaker SW, Monack DM. 2015. Cutting edge: inflammasome activation in primary human macrophages is dependent on flagellin. J Immunol 195:815–819. https://doi.org/10.4049/jimmunol.1403100.
26. Jurk M, Heil F, Vollmer J, Schetter C, Krieg AM, Wagner H, Lipford G, Bauer S. 2002. Human TLR7 or TLR8 independently confer responsive-

ness to the antiviral compound R-848. Nat Immunol 3:499. https://doi.org/10.1038/ni0602-499.
27. Bhatia HK, Singh H, Grewal N, Natt NK. 2014. Sofosbuvir: a novel treatment option for chronic hepatitis C infection. J Pharmacol Pharmacother 5:278–284. https://doi.org/10.4103/0976-500X.142464.
28. Guilliams M, Ginhoux F, Jakubzick C, Naik SH, Onai N, Schraml BU, Segura E, Tussiwand R, Yona S. 2014. Dendritic cells, monocytes and macrophages: a unified nomenclature based on ontogeny. Nat Rev Immunol 14:571–578. https://doi.org/10.1038/nri3712.
29. Fung-Leung WP, Kündig TM, Zinkernagel RM, Mak TW. 1991. Immune response against lymphocytic choriomeningitis virus infection in mice without CD8 expression. J Exp Med 174:1425–1429. https://doi.org/10.1084/jem.174.6.1425.
30. Lehmann-Grube F. 1971. Lymphocytic choriomeningitis virus, 1st ed. Springer-Verlag, Vienna, Austria.
31. Majeti R, Chao MP, Alizadeh AA, Pang WW, Jaiswal S, Gibbs KD, Jr, van Rooijen N, Weissman IL. 2009. CD47 is an adverse prognostic factor and therapeutic antibody target on human acute myeloid leukemia stem cells. Cell 138:286–299. https://doi.org/10.1016/j.cell.2009.05.045.
32. De Veer MJ, Holko M, Frevel M, Walker E, Der S, Paranjape JM, Silverman RH, Williams BRG. 2001. Functional classification of interferon-stimulated genes identified using microarrays. J Leukoc Biol 69:912–920.
33. Kojima Y, Volkmer J-P, McKenna K, Civelek M, Lusis AJ, Miller CL, Direnzo D, Nanda V, Ye J, Connolly AJ, Schadt EE, Quertermous T, Betancur P, Maegdefessel L, Matic LP, Hedin U, Weissman IL, Leeper NJ. 2016. CD47-blocking antibodies restore phagocytosis and prevent atherosclerosis. Nature 536:86–90. https://doi.org/10.1038/nature18935.
34. Betancur PA, Abraham BJ, Yiu YY, Willingham SB, Khameneh F, Zarnegar M, Kuo AH, McKenna K, Kojima Y, Leeper NJ, Ho P, Gip P, Swigut T, Sherwood RI, Clarke MF, Somlo G, Young RA, Weissman IL. 2017. A CD47-associated super-enhancer links pro-inflammatory signalling to CD47 upregulation in breast cancer. Nat Commun 8:14802. https://doi.org/10.1038/ncomms14802.
35. Banerjee R, Khandelwal S, Kozakai Y, Sahu B, Kumar S. 2015. CD47 regulates the phagocytic clearance and replication of the Plasmodium yoelii malaria parasite. Proc Natl Acad Sci U S A 112:3062–3067. https://doi.org/10.1073/pnas.1418144112.
36. Ayi K, Lu Z, Serghides L, Ho JM, Wang JCY, Liles WC, Kain KC. 2016. CD47-SIRPα interactions regulate macrophage uptake of *Plasmodium falciparum*-infected erythrocytes and clearance of malaria *in vivo*. Infect Immun 84:2002–2011. https://doi.org/10.1128/IAI.01426-15.
37. Su X, Johansen M, Looney MR, Brown EJ, Matthay MA. 2008. CD47 deficiency protects mice from lipopolysaccharide-induced acute lung injury and Escherichia coli pneumonia. J Immunol 180:6947–6953. https://doi.org/10.4049/jimmunol.180.10.6947.
38. Navarathna DHMLP, Stein EV, Lessey-Morillon EC, Nayak D, Martin-Manso G, Roberts DD. 2015. CD47 promotes protective innate and adaptive immunity in a mouse model of disseminated candidiasis. PLoS One 10:e0128220. https://doi.org/10.1371/journal.pone.0128220.
39. Nath PR, Gangaplara A, Pal-Nath D, Mandal A, Maric D, Sipes JM, Cam M, Shevach EM, Roberts DD. 2018. CD47 expression in natural killer cells regulates homeostasis and modulates immune response to lymphocytic choriomeningitis virus. Front Immunol 9:2985. https://doi.org/10.3389/fimmu.2018.02985.
40. Feng M, Chen JY, Weissman-Tsukamoto R, Volkmer J-P, Ho PY, McKenna KM, Cheshier S, Zhang M, Guo N, Gip P, Mitra SS, Weissman IL. 2015. Macrophages eat cancer cells using their own calreticulin as a guide: roles of TLR and Btk. Proc Natl Acad Sci U S A 112:2145–2150. https://doi.org/10.1073/pnas.1424907112.
41. Steeves RA, Mirand EA, Thomson S, Avila L. 1969. Enhancement of spleen focus formation and virus replication in Friend virus-infected mice. Cancer Res 29:1111–1116.
42. Moriarty TJ, Norman MU, Colarusso P, Bankhead T, Kubes P, Chaconas G. 2008. Real-time high resolution 3D imaging of the Lyme disease spirochete adhering to and escaping from the vasculature of a living host. PLoS Pathog 4:e1000090. https://doi.org/10.1371/journal.ppat.1000090.
43. Sambandamurthy VK, Derrick SC, Jalapathy KV, Chen B, Russell RG, Morris SL, Jacobs WR, Jr. 2005. Long-term protection against tuberculosis following vaccination with a severely attenuated double lysine and pantothenate auxotroph of Mycobacterium tuberculosis. Infect Immun 73:1196–1203. https://doi.org/10.1128/IAI.73.2.1196-1203.2005.
44. Newman AM, Liu CL, Green MR, Gentles AJ, Feng W, Xu Y, Hoang CD, Diehn M, Alizadeh AA. 2015. Robust enumeration of cell subsets from tissue expression profiles. Nat Methods 12:453–457. https://doi.org/10.1038/nmeth.3337.
45. Blanco-Melo D, Nilsson-Payant BE, Liu W-C, Møller R, Panis M, Sachs D, Albrecht RA, tenOever BR. 2020. SARS-CoV-2 launches a unique transcriptional signature from in vitro, ex vivo, and in vivo systems. bioRxiv 2020.03.24.004655. https://doi.org/10.1101/2020.03.24.004655.
46. Mei HE, Leipold MD, Maecker HT. 2016. Platinum-conjugated antibodies for application in mass cytometry. Cytometry A 89:292–300. https://doi.org/10.1002/cyto.a.22778.